DOI: 10.4408/IJEGE.2021-01.S-10

AN ALTERNATIVE TO COMMERCIAL OPTICAL FIBRE SENSORS FOR SHALLOW LANDSLIDE MONITORING – INTERFEROMETRIC OPTICAL FIBRE SENSING

Vladislav IVANOV(*), Maddalena FERRARIO(**), Marco BRUNERO(**), Monica PAPINI(*) & Laura LONGONI(*)

(*)Politecnico di Milano - Dipartimento di Ingegneria Civile e Ambientale - 20133 Milano (Italy)
(**)Politecnico di Milano - Dipartimento di Elettronica, Informazione e Bioingegneria - Via Giuseppe Ponzio, 34 - 20133 Milano (Italy)
Corresponding author: laura.longoni@polimi.it

EXTENDED ABSTRACT

I sensori in fibra ottica hanno ormai assunto un ruolo importante nel monitoraggio del dissesto idrogeologico. Il monitoraggio con la fibra ottica offre delle nuove potenzialità nel monitorare processi di allungamento e/o cambio di temperatura, che a loro volta potrebbero indicare l'occorrenza di eventi franosi. Attualmente, a seconda della tecnologia di acquisizione, i sensori in fibra ottica offrono una misura distribuita con una risoluzione spaziale nell'ordine del microstrain lungo diversi chilometri di distanza e una frequenza di acquisizione fino al MSample/s. In aggiunta, un ulteriore vantaggio nell'utilizzare le fibre ottiche è il basso costo del sensore, l'immunità ai campi magnetici e la durabilità.

Nei due decenni passati varie applicazioni, con l'uso di differenti sensori in fibra ottica, hanno mostrato l'avanzamento di questa tipologia di monitoraggio come potenziale sostituto degli strumenti di monitoraggio convenzionali, come ad esempio gli inclinometri. Nonostante ciò, il monitoraggio basato sulle fibre ottiche è ancora in fase di sviluppo e ancora non sostituisce completamente i sistemi tradizionali.

Le potenzialità dei sensori in fibra ottica nell'ambito del dissesto idrogeologico sono maggiormente sfruttate per il monitoraggio di fenomeni franosi caratterizzati da tempi di sviluppo relativamente lenti. Le misure ottenute sono principalmente la deformazione (strain) della fibra ottica, dovuta alla deformazione del versante. Pochi studi hanno tentato di sfruttare le potenzialità di questa tecnologia nel rilevare i segnali dovuti alla propagazione delle onde elastiche causata dalla deformazione del terreno. Tali segnali potrebbero indicare l'innesco di fenomeni franosi che sono tipicamente privi di segni premonitori, come per esempio le frane superficiali.

Negli studi che si sono focalizzati sul monitoraggio di questo fenomeno tramite i sensori in fibra ottica, vari autori hanno simulato l'innesco di frane superficiali/colate di detrito a scala di laboratorio. I risultati riportati evidenziano una buona capacità dei sensori di rilevare dei segnali considerati premonitori del collasso vero e proprio. Nonostante i risultati promettenti, questi studi coinvolgono degli interrogatori ottici che sono caratterizzati da un costo molto elevato, nell'ordine di 80-100 mila €, che potrebbe essere un ostacolo importante nell'applicare un sistema di monitoraggio di questo tipo in sito.

In questo studio, gli autori propongono un sensore in fibra ottica interferometrico che, nonostante il suo design semplice, si presenta efficace nel rilevare gli strain di diversi ordini di grandezza. L'ingegnosità del suo design lo rende poco dipendente dalla qualità del laser di sorgente che a sua volta permette di abbassare notevolmente i costi della sua messa in opera. Per verificarne le potenzialità nel rilevare i segnali precursori dell'innesco di una frana superficiale, gli autori propongono quattro prove di laboratorio nelle quali sono state simulate frane indotte da precipitazioni intense. I corpi frana sono stati attrezzati con i sensori sopraindicati. I diversi test coinvolgono diversi compositi di materiale granulare (sabbia e ghiaia) e una diversa impostazione dei sensori all'interno del terreno. I segnali ottenuti sono stati processati nel dominio delle frequenze tramite l'analisi spettrale di tipo multi-taper che permette di seguire la variazione del contenuto spettrale nel tempo per la durata della prova fino al collasso.

Per confrontare l'andamento dello spettro con il comportamento del corpo frana, sono sati stimati gli spostamenti superficiali tramite digital image correlation (DIC), effettuata su immagini consecutive scattate durante l'esecuzione delle prove.

I risultati ottenuti confermano le capacità del sensore interferometrico di riflettere le diversi fasi di sviluppo di instabilità nel terreno tramite la variazione del contenuto spettrale rilevato. Le prove che coinvolgono materiale più grossolano dimostrano un contenuto spettrale maggiormente energetico. Il confronto con le misure del movimento superficiale evidenziano la concomitanza dell'accelerazione del terreno con il picco dell'intensità del contenuto spettrale, mentre i primi segni di instabilità vengono indentificati dai sensori diversi minuti prima del collasso, quando il movimento rilevato sulla superficie è ancora minimo.

L'esito di queste prove certifica l'applicabilità di questo sensore in fibra ottica per il monitoraggio di frane superficiali indotte da precipitazioni intense. Il rilevamento di segnali premonitori di instabilità fornisce degli indicatori quantitativi che potrebbero essere ulteriormente integrati con sistemi di early warning basati sul rilevamento dell'intensità e durata delle precipitazioni.

ABSTRACT

Optical fibre-based monitoring has settled in the field of geohazards monitoring. Interferometric optical fibre sensors are the least used in landslide monitoring, while classical approaches rely on Fibre Bragg Grating and Brillouin Optical Time Domain Reflectometry/Analysis. Landslide monitoring goes hand by hand with the development of technology. While authors tend to focus on the unprecedented accuracy and reduced costs of the sensor itself, the economic and practical aspects related to the interrogating systems are often disregarded. Recently, a simpler and significantly more cost-effective approach has been introduced through "integral coherent measurements" because they yield an integral of the signal response over the entire length of the optical fibre sensor. This sensing system proves to be suitable to provide an overall indication of the state of the entire monitored domain and yield indications of the onset of motion with a high temporal resolution. The sensor has been tested in controlled conditions as a monitoring tool in a downscaled landslide model. We exploit the large bandwidth and high frequency of acquisition in order to detect high frequency elastic waves. The proposed sensor is able to distinguish the vibration footprint generated by ground movement. The results obtained from the experimental tests demonstrate that the proposed sensing system is able to recognize the onset of motion some minutes before a visual indication of instability could be observed.

Keywords*: Optical fibre sensing, acoustic emissions, shallow landslides, laboratory simulations, multi taper spectral analysis*

INTRODUCTION

Optical fibre sensing, successfully applied to geohazard monitoring has been demonstrated through a broad range of applications, involving a variety of slope stability issues (Schenato, 2017). In most general terms, an optical fibre's physical deformation, or local temperature change induce a respective change in the light signal propagating within the cable's core. The detection of this change allows for the monitoring of ground movement with unprecedented spatial and temporal resolutions. A detailed review on the basic concepts and applications have been summarized in the works of Schenato (2014) and Schenato (2017). The potential of optical fibre sensors has been well exploited in monitoring slope stability, both in the laboratory and through in situ applications. The majority of applications involve coupling an optical fibre sensor cable to a carrier (e.g., an inclinometer casing) which transmits the slope deformation to a coated optical fibre. Other common monitoring applications include the direct ground burial of the monitoring cables as well as their coupling to geotechnical reinforcements. Distributed sensing through Brilloiun Optical Time Domain Reflectometry/Analysis (BOTDR/A) is preferably employed as it returns as output a distributed sensing profile of the respective measurand, although single-point sensors based on Fibre Bragg Gratings (FBGs) installed in series are common as well. The measurand in more than two thirds of the applications is the strain induced on the sensor or a simultaneous measure of strain and temperature. Optical fibre vibration sensing has only recently been considered for landslide monitoring through several applications in which the high sensor sensitivity allows for the detection of the high frequency elastic waves on the sensing unit (Huang *et alii*, 2012; Rajan *et alii,* 2016; Michlmayr *et alii*, 2017). In terms of monitored phenomena, optical fibre sensing has rarely been employed for rainfall induced landslides. The swift development and limited signals of instability related to such slides render their monitoring a challenging task. Picarelli *et alii* (2015), Schenato *et alii* (2017) carried out experimental landslide simulations of rainfall induced slides equipped with optical fibre sensors, while Michlmayr *et alii* (2017) simulated a relatively coarse debris-like slope failure. Those works demonstrated that optical fibre sensors can be viable tools for shallow ground stability monitoring. The distributed sensing schemes used by the majority of authors are based on commercially available technology, typically designed for purposes different from ground monitoring, and with relative interrogator costs of ranging between €80k - €100k. A recently revived optical fibre sensing technology is based on Michelson's interferometer. Its simple but efficient design, based on a separate sensing and reference fibre, renders it less dependent on the quality of the input laser source and thus ensures large sensing bandwidths and high sampling frequency without the need for a narrow linewidth, which accrues the major portion of the interrogator costs. Such has been successfully applied in a couple of direct strain applications in the past in both in-situ applications by Bruckl *et alii* (2013) and Lienhart (2015) and laboratory experiments by Papini *et alii* (2020) and Ivanov *et alii* (2021). In this work, instead, we propose the application of an interferometric optical fibre sensor for vibration sensing in a model slope of granular material. We present the results of four experiments in which the slope is equipped with optical fibre sensors in different configurations. We process the obtained sensing signals in the frequency domain, by means of a multi-taper spectral analysis. We compare the trends in the frequency spectrum detected during the experiments to surface displacement fields estimated through digital image correlation (DIC) of consecutive images of the model slope during the experiments.

The main goals of this work are (1) to verify the applicability of the previously described optical fibre sensors for landslide monitoring and (2) to exploit the large bandwidth and high sampling frequency for the identification of instability precursors in what is typically a swiftly developing process.

EXPERIMENTAL SETUP AND CONDUCT

The experimental work was carried out in the laboratory of Applied Geology and Mountain Hydraulics in the Lecco Campus of Politecnico di Milano. A 2m by 0.8m steel structure flume with a modifiable inclination was designed for the landslide simulations (Fig. 1). Its inclination could be increased up to 45°. The flume was exploited for the execution of a number of experiments with different goals such as the investigation of the effect of different hydrological parameters on the onset of shallow slope failures (Ivanov *et alii*, 2020), testing geophysical and photogrammetric instrumentation in the context of landslide monitoring (Arosio *et alii*, 2018; Scaioni *et alii*, 2018; Hojat *et alii*, 2019; Hojat *et alii*, 2020) and ultimately optical fibre sensors (Papini *et alii*, 2020; Hojat *et alii*, 2021).

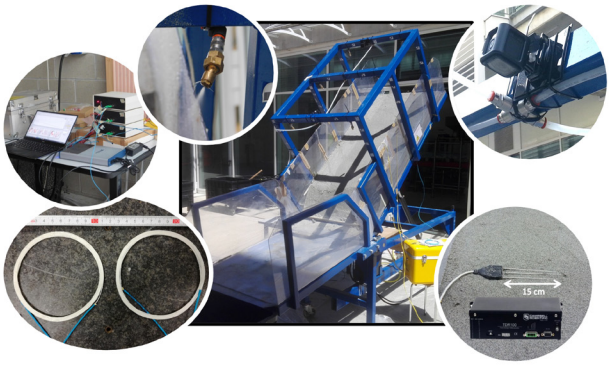

Fig. 1 - Experimental setup. Centre – inclined flume containing the landslide material. Left from top to bottom – sprinkler for rainfall simulation, optical fibre sensors' interrogating units and PC, optical fibre sensing coils. Right – Action camera and TDR probe.z

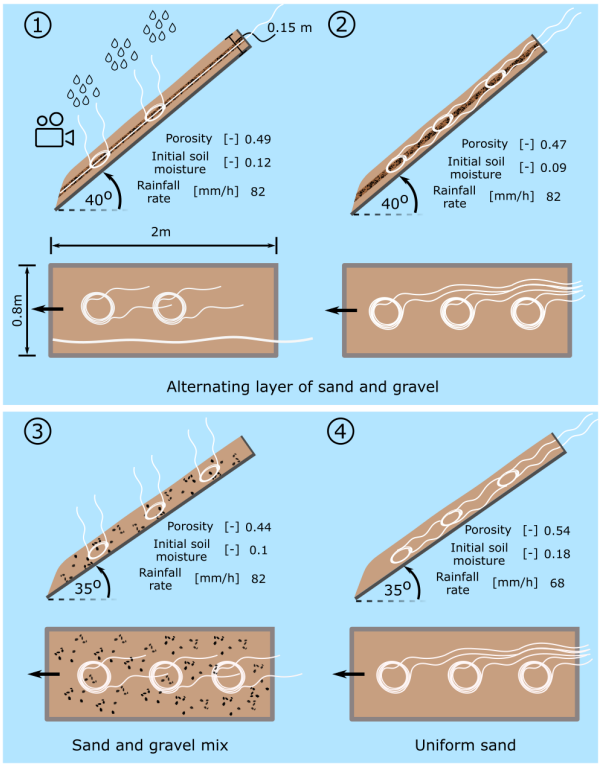

Fig. 2 - Experimental setup of the four tests. Plan view of the experimental setup is illustrated in the upper row of images, while the lower row represents a side view. The location and different mode of deployment of the optical fibre sensors is illustrated in the images. D, M, U, and L stand for downslope, midslope, upslope and longitudinal, respectively. Values of porosity, initial soil moisture, rainfall rate and dip angle are reported in the image. The different soil composition is represented schematically and indicated above each section image

In this work, a set of 4 experiments was carried out. They differ in the modality of sensors placement, the soil mixture involved, the hydrogeological parameters of the mixture, the slope dipping angle, and the simulated rainfall event. Those parameters are summarized in Fig. 2. In experiment 1, alternating layers of sand and gravel were created, and the sensors were placed within the gravel layer while their leading cables protrude directly from the soil surface. Two coil sensors and one longitudinally placed sensor were installed. In experiment 2, the same layered setup was used but with three coil sensors, while sensor leads remained buried within the soil. Experiment 3 featured a mixture of sand and gravel, three coil sensors with sensor leads protruding from the surface. Experiment 4 has a setup similar to the one of experiment 2, however the landslide body is composed of uniform sand. The different setups are schematically represented in Fig. 2.

Soil was placed in the flume in layers with uniform compaction that was ensured by fitting a known mass of soil to a certain volume in the channel. The soil samples were compacted using wooden boards over which weight was applied until a given mass of terrain fitted the predefined volume. The depth of the soil layer was set to 15 cm in all 4 experiments. Initial soil moisture content was measured and adjusted to a predefined value at the beginning of the experiment. The coils in this case were installed in the gravel layer in order to attempt to enhance the impact of failing soil on the sensors. Sensor leads were left free to protrude from the surface of the slope in order to avoid then being strained. After the terrain was settled, the upper platform was lifted to form the desired inclination. Rainfall was then initiated and controlled to maintain a constant value through a pressure control valve. Fig. 3 illustrates the failure captured during experiment 3 as an example. A failure pattern could be outlined through inspection of the images collected by the cameras: first, seepage was observed near the toe of the slope. This was followed by toe erosion and consecutive detachment of soil chunks in a retrogressive manner. First

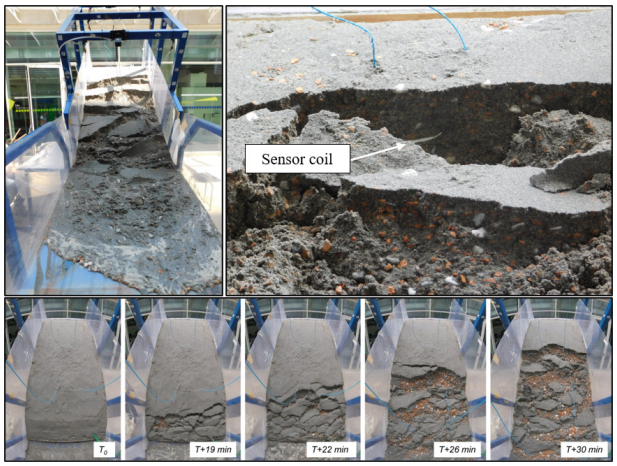

Fig. 3 - Left - Runout during the collapse of experiment 3. Right – close up of a coil sensor involved in the collapse process. Bottom - Image sequence illustrating the development of experiment 1. The intervals between frames are indicated in the lower right corner

failures occurred at the downslope end of the landslide body, typically preceded by the aperture of a crack which grew in size progressively. While in experiment 1, 2 and 3 soil block detachment manifested rather plastic flow-like sequence, during experiment 4 detachments of sand portions were abrupt and somewhat brittle. The imminence of failure typically set in about 15-20 minutes into the experiment and runout continued up until 30 mins from the start. TDR measurements indicated that first failures occurred at full or nearly full saturation of the slope at the section where the TDR was placed. An image sequence of the previously described process is illustrated in Fig. 3. Surface displacement was tracked through DIC, where possible. The uniform texture of the landslide surface was, in some portions of the slope, hardly suitable for the software to carry out the processing. Estimations of surface displacements are thus available mostly for the lower and middle sections of the landslide body. Considering that those are the locations where first failures occurred, we consider this limitation to be insignificant. Due to a technical issue, the recording of the optical fibre sensor signals started 6 minutes after the start of rainfall. Therefore, the following plots relative to this experiment have a blank space for the first 6 minutes.

OPTICAL FIBRE SENSING AND DATA ANALYSIS

Optical fibre sensor

The coherent fibre optic sensing solution exploited in this work relies on a novel phase-diversity coherent detection scheme (Martinelli & Ferrario, 2013) which combines a 3x3 optical coupler with standard optical fibres terminated with Faraday rotator mirrors (FRMs). A distributed feedback laser (DFB) is coupled to one input of the 3x3 coupler, the optical signal is split and sent through both reference and sensing arms. In the sensing arm, the interaction of the measurand (effectively, any perturbations which occur at the subsurface) with the sensing fibre, results in a perturbation of the phase, $\Delta\theta t$, of the propagating optical signal. The phase variation, $\Delta\theta t$, is then recovered by registering the interference between the optical signals, back reflected by the FRMs, inside the 3x3 coupler. The resulting interference signals are then detected by a pair of photoreceivers (Boffi *et alii*, 2009). The sensing scheme is defined as "integral" as each single measurement provides the integral of the phase difference gained by the optical signal during its propagation along the entire length of the sensing cable ($\Sigma\Delta\theta(t)$). Since the experiments carried out here aim at identifying high frequency impact on the sensing cables, the sampling frequencies were set to 10 kSamples/s in experiments 1 and 2, and 25 kSamples/s in experiments 3 and 4.

The integral phase difference, $\Sigma\Delta\theta(t)$, recorded during the experiments was processed in order to identify the most significant stages of instability development. A highpass filter (0.9 Hz) was applied in order to remove low frequency oscillations which are hardly interpretable. The resulting signal was processed by means of time-frequency analysis which involved the analysis of the frequency spectrum of the signal in sequential and overlapping time windows. This allowed for the inspection of the spectral content up to the Nyquist frequency – 5kHz for experiments 1 and 2, and 12.5 kHz for experiments 3 and 4.

Data processing

The spectral analysis was carried out following the approach defined as multitaper spectral analysis. The approach is based on the work of Prerau *et alii* (2017), who applied the technique to the analysis of oscillatory dynamics data gathered in an electroencephalogram (EEG) and regarding sleep quality. While the application might be entirely different, the method is said to provide a robust estimation of the spectral content, reducing the bias and variance with respect to periodogram-based estimates. The described procedure is implemented in a MATLAB code, readily available for use at: https://prerau.bwh.harvard.edu/multitaper/.

The raw signals obtained by the optical fibre sensors can hardly be interpreted in the time domain. In particular, the low frequency oscillations due to the cable swinging or deformation potentially mask what is the high-frequency response of the sensors due to micro deformations, settlement, swelling, or water infiltration – effects which could be considered to be precursors of the onset of instability. The simplest method for spectral estimation is the computation of the periodogram, which involves the application

of the fast Fourier Transform. However, the periodogram is characterized by features that could cause different biases related to the main and side lobes of the spectral estimate. The side lobes are associated with a broadband bias, or the introduction of noise across a band of frequencies in the estimate. Therefore, the power which belongs to a given frequency is distributed erroneously to other frequencies in the spectrum. On the other hand, the main lobe blurs all frequencies within the range of its bandwidth – if two oscillations are separated by a frequency that is smaller than the width of the lobe, they will be interpreted as one single oscillation. The width of the main lobe therefore defines the spectral resolution of the estimate, or the smallest distinguishable difference in frequency. A common method for dealing with the aforementioned issues is the application of a tapering window function before carrying out the spectral estimation. This results in what is defined as single-tamper spectrum. Since the main and side lobes of the periodogram are consequences of the sharp changes in the start and end of the data, tapering functions that have a gradual transition between one and zero decrease the power in the side lobes of the spectrum, while the prominence of the main lobe is increased. Less power leaking results in less biased estimate. Typical tapers include Hanning, Hamming, Blackman, Gaussian and Welch functions. However, while tapering reduces bias, it can be the cause for an increased variation as it forces the time points near the ends to converge to zero, which reduced the amount of data available for the estimate.

To confront this issue, a technique known as the multitaper method (Thomson, 1982) that has been demonstrated to be superior in comparison to the single-taper spectral estimate. It works by averaging several independent single-taper spectra originating from the same portion of data. Several parameters define the outcome of this analysis: N [s], the size of the data segment, or the temporal resolution; f [Hz], the frequency resolution, and L [-] the number of tapers used. There is a trade-off between temporal and frequency resolutions in what an increase in one inevitably lessens the other, while for each combination of N, and f, there exist an optimal number of tapers, L that yield the best performing spectrogram.

Displacement estimation

The sequential images taken during the experiments were further used in a digital image correlation (DIC) software (GOM Correlate, https://www.gom.com/index.html) in order to estimate surface displacements of the soil mass at specified points. GOM Correlate is a DIC evaluation software used for a variety of purposes involving strain and displacement, and velocity inspection and evaluation, typically with reference to mechanical components. The software creates a surface component on which displacement fields are estimated. While establishing the surface component, the software finds square-shaped facets in the collected scenes. The software identifies these facets by the stochastic pattern quality structure. While typically an ad-hoc recognizable pattern would be required to cover the analysed area and enhance the recognition algorithms, it also works well with natural patterns such as the sand that we use during the land sliding experiments.

The software has been successfully applied for the detection of landslide displacement using high resolution satellite images (Caporossi *et alii*, 2018). The scale of the experimental setup here is clearly much different. Nonetheless, since the application of the software provides a subpixel precision, it has been considered a suitable tool for the estimation of the displacement fields of the sand body. The surface displacements were therefore compared to the results obtained from the optical fibre sensors in order to understand what the state of the landslide is, once the sensors evidence potential disturbance in the subsurface.

RESULTS

As a first step, a sensitivity analysis (Fig. 4) is carried out to explore the effect of the number of tapers, and the consequent temporal and frequency resolutions on the resulting spectrograms. This analysis is carried out on sensor L of experiment 1. The frequency range is limited to 500Hz as the spectral content above this value does not seem to be particularly energetic (not shown).

The sensitivity analysis illustrates how the parameters used for the definition of the spectral analysis impact its results. The initial assumption of having a high temporal resolution (0.1s) and a large number of tapers (9) led to the results presented on the top plot. Those parameters lead to a frequency resolution of 100Hz. While here we are more interested in the temporal development of the process rather than its spectral footprint, it can be noticed that this low frequency resolution creates a discontinuity in the

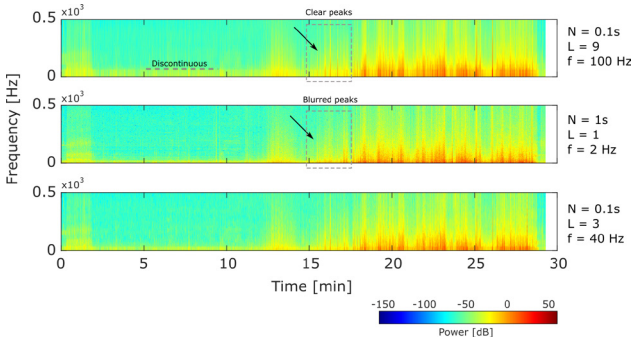

Fig. 4 - A sensitivity analysis on the spectral analysis parameters, reported on the left side of the plots. N = temporal resolution, f = frequency resolution, L = number of tapers

estimation of the power of neighbouring frequencies. While in terms of visual representation this might be acceptable, the further analysis of estimating the cumulative band power could

be affected. Increasing the frequency resolution to 2 Hz (at the expense of a decreased temporal resolution of 1s), it can be noticed that the spectral estimation is more continuous along the frequency axis. However, this leads to a single taper estimate (L=1) as a necessary condition. Moreover, some of the peaks estimated previously (grey rectangles) are somewhat averaged with neighbouring data due to the larger temporal window. This might be problematic in what such peaks could be interpreted as precursors. Therefore, the temporal resolution used in the first example (N=0.1s) will be restored, while in order to act on the low frequency resolution, the number of tapers is set to L=3, and the frequency resolution f=40 Hz. The result appears to be reasonable both in terms of frequency and time, as no loss of peaks or 'events' is present here and the power spectrum is not discontinuous as in the first example. This configuration will therefore be used in the consecutive analysis. Figs 5 and 6 illustrate the results of this processing, limited in frequency to 500 Hz. The collapse instants are marked by red arrows and refer to the collapses that correspond to the particular sensor. Their correspondence to peaks in the power spectrum is immediate.

The longitudinally placed sensor reflects the entire runout process since its beginning. A preliminary phase can be outlined as well, which corresponds to a spring-like seepage at the toe of the slope.

The failure episodes recorded by the downslope and midlsope sensors continue until the sensor remains uncovered and thus two distinct episodes can be distinguished here. In experiment 2 instead, where the sensor leads are buried as well, monitoring continues even after the failure of the soil over the coil. The upslope sensor is rarely involved in any direct collapse. This is evident in all experiments 2, 3, and 4 since no clear energy peak can be outlined on the plots related to those sensors. On the other hand, there is an energetic footprint limited up to around 100 Hz, which becomes more pronounced towards the end of the experiment, and therefore corresponds to the retrogressive advancement of slope failure. Distinct 'event' can be outlined in experiments 2,3 and 4 which were reflected by all three sensors. In experiment 2 those can be attributed to an external disturbance. In experiment 3 the failure in the toe of the slope was sensed also by the midslope and upslope sensors. In experiment 4, several abrupt detachments of soil occurred in the toe of the slope marked by the respective peaks in all of the plots related to this experiment. The initial phase of experiment 3 is characterized by a high energy signal response over the entire range up to 500 Hz.

A dominant frequency can be noticed here at around 400 Hz. Its origin might be attributed to the direct impact of rainfall on the sensor's leads, which remained uncovered. Even though the peaks related to the distinct collapses are quite distinct (especially in the downslope sensor of experiment 4),

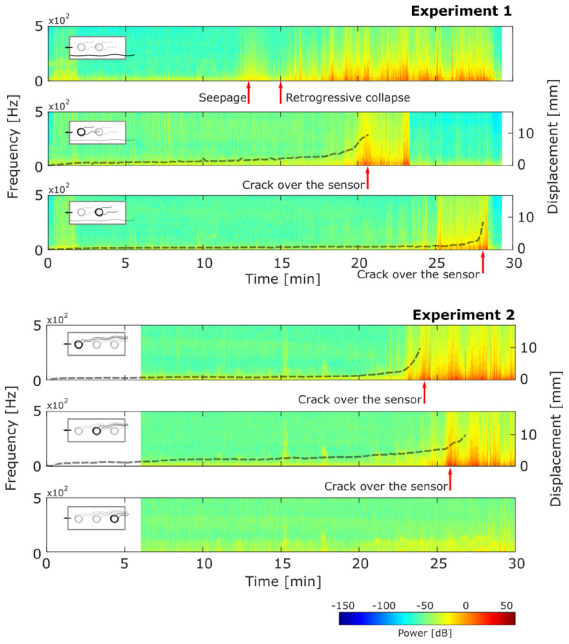

Fig. 5 - Multi -taper spectral estimation for the sensors of experiments 1 and 2. The spectra are limited to 500Hz. The insets in the different plots indicate the sensor which the spectral estimate refers to. The red arrows indicate distinct collapses

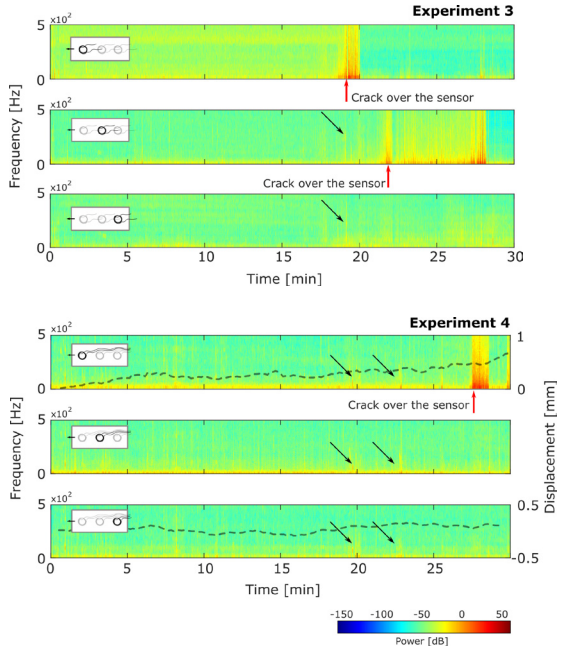

Fig. 6 - Multi -taper spectral estimation for the sensors of experiments 3 and 4. The spectra are limited to 500Hz. The insets in the different plots indicate the sensor which the spectral estimate refers to. The red arrows indicate distinct collapses

it can be noticed that there is an increase of the energy in the spectral content some time before the actual collapse occurs.

This is distinguishable from the predominantly bright yellow colour preceding the collapse event. This can be associated to a precursory phase that indicates the onset of instability in the vicinity of the sensor.

The estimated displacements illustrate the state of mobility of the landslide body during the experiments. In comparison with the spectral content estimates, one can identify the correspondence between the acceleration of the slope and the increase in the spectral power. This is particularly evident in experiments 1 and 2 where the peak in the spectral power occurs simultaneously with the highest recorded slope movement of around 10 mm (after which the traced soil surface slips away from the field of observation). It can be further noticed that, at very low displacement values (1-2 mm) there is an increase in the power of the spectral content, which precedes the actual collapse of the slope. This is a clear precursor of the onset of instability which occurs at the subsurface, while at the surface, there is little indication of the development of this process. Unfortunately, displacement tracing was impossible for experiments 3 and 4. However, some signals preceding the collapse are visible, especially with reference to the midslope sensor. Experiment 4 demonstrates an entirely different behaviour. The uniform landslide body behaved in a rather rigid manner, with no "plastic" and continuous failure as in the previous experiments. Rather, here the failure was a sequence of abrupt detachments of chunks of soil clearly marked by the peaks in spectral power.

DISCUSSIONS

The results obtained from the experimental tests demonstrate that the optical fibre sensors are able to reflect the development of instability within the soil body. Sensor positioning appears to be rather important as single-point sensors are most effective in reflecting the slope dynamics in the vicinity of the sensor itself, while the longitudinally installed sensor revealed the evolution of slope mobilization from the first instants of toe seepage to the runout phase. The proposed interferometric optical fibre sensors yielded a rather high sensitivity to the perturbances which occurred within the soil body. The recorded footprint is most pronounced up to 500 Hz although during failure the spectral power increases in the entire frequency range up to 12.5 kHz (not shown). Particularly useful is the ability of the sensors to reflect precursors of instability evidenced by the increase in the power of the spectral content before the collapse occurs. In some cases, precursors can be outlined several minutes in advance, although a more extensive analysis would be required to precisely quantify this window. What could tentatively be outlined as warning periods are comparable in terms of duration to similar studies on detection of acoustic emissions AE in granular material. Michlmayr *et alii* (2017) reported a precursory window of 100 s before failure even though in this work, the precursors are accompanied by isolated collapses, which could be visually identified as well. Instead, Hu *et alii* (2018) report an increase in acoustic emissions and micro seismic rates as early as 50 s prior to failure. In the cited work however, apart from the different sensors, the simulated failure mechanism is rather different in what the landslide failure was not rainfall-induced but occurred by gradual slope saturation. Both those experiments featured a sediment mixture characteristic of debris flow with a combination of fine and coarse material. Similarly to our work, some authors report the use of coarse material as a way to enhance the generation of more energetic signals. For instance, Deng *et alii* (2019) presented a displacement-driven downscaled slope failure where the source of AE is the gravel backfill of an inclinometer casing coupled to a piezoelectric sensor. The authors report to have been able to derive links between increments of displacement and the recorded acoustic emission signal. Similar works featuring waveguides for AE signal amplification at the laboratory scale was carried out by Smith *et alii* (2014, 2017) who identified a correlation between subsurface deformation and AEs even at velocities in the order of 0.3 mm/hr. Field applications of the same waveguide-based system was proposed by the same authors. Here the recorded AE were linked to the displacement of a landslide along a shear zone (Dixon *et alii*, 2003, 2015, 2018). In our experiments, a failure surface is designated a priori, that is, the control over the process is purely hydrologic. We did not consider a waveguide necessary as the sensors are merely optical fibre cables that could be placed in direct contact with the soil mixture. Placement of sensors directly in the landslide body, and in particular, a distributed optical fibre coil-like sensors, based on BOTDA is featured in Michlmayr *et alii*, 2017.

The aforementioned authors used an interrogating technology characterized by an extremely high sampling frequency. However, such an instrument might be impractical for applications outside the laboratory due to high cost of the interrogating unit. The cost of the interferometric sensor adopted in this work is in the order of few thousands of euros. If combined to an optical switch to multiplex N fibre sensors, the overall cost could reach around €5k which is indeed much cheaper with respect to commercially available distributed sensors, the cost of which has decreased in recent years but still remains high at around €80k-100k.

Although simpler, the interferometric sensor that we used in this work, does not yield to BOTDA/R sensing schemes in terms of bandwidth and frequency of acquisition. The sensing scheme features a wide acquisition bandwidth capability, up to the MHz, limited only by the Analog-to-Digital Converter (ADC) sampling board (Sbarufatti *et alii*, 2017). In the presented experiments the sampling frequency of the interferometric sensor, up to 25 kSample/s was wide enough to capture variations in the frequency range of up to 12.5 kHz. The integral nature of the presented interferometric approach is surely a shortcoming as it does not allow to localize the origin of strain along the fibre length,

contrarily to distributed fibre optic monitoring systems which yield the entire strain profile in detail along the sensing cable with centimetre spatial resolution (e.g., Papini *et alii*, 2020). This limitation can, however, be overcome by adding a multiplexing functionality to the interferometric interrogator so that tens of sensing fibre sections could be exploited to cover the entire area of interest. Alternatively, two integral interferometric sensors can be exploited in a counter-propagating scheme allowing for event localization as recently demonstrated by Di Luch *et alii* (2019). The authors acknowledge that moving from the laboratory to full-size application might not be a straightforward task.

Difficulties accompanying vibration sensing include strong signal attenuation in heterogeneous and saturated materials (Faillettaz *et alii*, 2016) as well as signal source localization. In the interferometric optical fibre sensing proposed here we see a step forward towards overcoming the aforementioned issues. Particularly valuable is the possibility to monitor an extended area at a reasonable installation and operational costs. Nevertheless, the real scale application of this monitoring system is yet to be tested and remains a challenging task. The results obtained here indicate that a precursory phase of variable duration (typically a few minutes) can be outlined during the experiments. A common question arising in downscaled model simulations is related to the correspondence between the timescales of the simulations and that of a potential full-size phenomenon. Iverson (2015) stated that the larger the experimental setup is, the weaker the possible scale effects will be, with reference to the velocity of a moving landslide body. For what concerns the infiltration and redistribution of water, the velocity of the process will likely be controlled by the dimensions of the landslide body, its composition in terms of granulometric distribution, as well as the rainfall rates causing the failure. Considering the limited thickness of the model (0.15 m) and its potential full-scale counterpart (shallow landslide depth <2 m), as well as the excessive rainfall rates simulated in the laboratory, a time scaling factor of more than 10 could be a reasonable approximation for a full-size phenomenon.

CONCLUSIONS

In summary, this work presented the results of a series of experimental tests, featuring the use of an interferometric optical fibre sensor as a monitoring tool in granular slope failures. The scope of the experiments was to identify precursors of failure through vibration sensing. Tests were carried out in a laboratory-scale physical model, where the landslide body was composed of different mixtures of sand and gravel. The optical fibre sensors were placed within the terrain under different configurations. Monitoring was accompanied by TDR measurements for direct observation of volumetric water content and time lapse image acquisition for surface displacement estimation through digital image correlation. We processed the recorded signals in the time-frequency domain through by means of multitaper spectral analysis in order to estimate the variation in the spectral content of the signal. The outcomes of the experiments can be summarized in the following:

- The interferometric optical fibre sensor proposed here was able to detect the different stages in the development of instability of the landslide body.
- Different sensor positions can be used to either concentrate sensing into a particular portion of the slope or to monitor an extended area during all phases of the instability development and runout.
- The interferometric optical fibre sensor introduced in this work, is a viable approach to obtain quantitative information on potential failure episodes. This information could complement existing early warning systems based, for instance, on rainfall intensity-duration thresholds.

REFERENCES

Arosio D., Hojat A., Ivanov V.I., Loke M.H., Longoni L., Papini M., Tresoldi G. & Zanzi L. (2019) - *A laboratory experience to assess the 3D effects on 2D ERT monitoring of river levees*. Paper presented at the 24th European Meeting of Environmental and Engineering Geophysics.

Boffi P., Ferrarese G., Ferrario M., Malavasi S., Mastronardi M.V., & Mattarei M. (2019) - *Coherent optical fiber interferometric sensor for incipient cavitation index detection*. Flow Measurement and Instrumentation, **66**: 37-43.

Brückl E., Brunner F., Lang E., Mertl S., Müller M. & Stary U. (2013) -*The Gradenbach Observatory—monitoring deep-seated gravitational slope deformation by geodetic, hydrological, and seismological methods*. Landslides, **10** (6): 815-829.

Caporossi P., Mazzanti P. & Bozzano F. (2018) - *Digital image correlation (DIC) analysis of the 3 December 2013 montescaglioso landslide (Basilicata, Southern Italy): Results from a multi-dataset investigation*. ISPRS International Journal of Geo-Information, **7** (9): 372.

Deng L., Yuan H., Chen J., Sun Z., Fu M., Zhou Y., Yan S., Zhang Z. & Chen T. (2019) - *Experimental investigation on progressive deformation of soil slope using acoustic emission monitoring*. Engineering Geology, **261**, 105295.

Di Luch I., Ferrario M., Brunero M., Boffi P., Beligni A. & Sbarufatti C. (2019) - *Coherent Fiber Optic Sensors for Impact Feature Assessment in Glass Fiber Reinforced Plastic (GFRP)*. Paper presented at the The European Conference on Lasers and Electro-Optics.

Dixon N., Hill R. & Kavanagh J. (2003) - *Acoustic emission monitoring of slope instability: development of an active waveguide system*. Proceedings of the institution of civil engineers-geotechnical engineering, **156** (2): 83-95.

Dixon N., Smith A., Flint J.A., Khanna R., Clark B. & Andjelkovic M. (2018) - *An acoustic emission landslide early warning system for communities in low-income and middle-income countries*. Landslides, **15** (8): 1631-1644.

Dixon N., Spriggs M., Smith A., Meldrum P. & Haslam E. (2015) - *Quantification of reactivated landslide behaviour using acoustic emission monitoring*. Landslides, **12** (3): 549-560.

Faillettaz J., Or D. & Reiweger I. (2016) - *Codetection of acoustic emissions during failure of heterogeneous media: New perspectives for natural hazard early warning*. Geophysical Research Letters, **43** (3): 1075-1083.

Hojat A., Arosio D., Ivanov V.I., Loke M.H., Longoni L., Papini M., Tresoldi G. & Zanzi L. (2020) - *Quantifying seasonal 3D effects for a permanent electrical resistivity tomography monitoring system along the embankment of an irrigation canal*. Near Surface Geophysics, **18** (Geoelectrical Monitoring), 427-443.

Hojat A., Arosio D., Ivanov V.I., Longoni L., Papini M., Scaioni M., Tresold G., & Zanzi L. (2019) - *Geoelectrical characterization and monitoring of slopes on a rainfall-triggered landslide simulator*. Journal of Applied Geophysics, **170**, 103844.

Hojat A., Ferrario M., Arosio D., Brunero M., Ivanov V.I., Longoni L., Madaschi A., Papini M., Tresoldi G. & Zanzi L. (2021) - *Laboratory Studies Using Electrical Resistivity Tomography and Fiber Optic Techniques to Detect Seepage Zones in River Embankments*. Geosciences, **11** (2): 69.

Hu W., Scaringi G., Xu Q. & Huang R. (2018) - *Acoustic Emissions and Microseismicity in Granular Slopes Prior to Failure and Flow-Like Motion: The Potential for Early Warning*. Geophysical Research Letters, **45** (19): 10, 406-410, 415.

Huang C.J., Chu C.R., Tien T.M., Yin H.Y. & Chen P.S. (2012) - *Calibration and deployment of a fiber-optic sensing system for monitoring debris flows*. Sensors, **12** (5): 5835-5849.

Ivanov V., Arosio D., Tresoldi G., Hojat A., Zanzi L., Papini M. & Longoni L. (2020) - *Investigation on the Role of Water for the Stability of Shallow Landslides—Insights from Experimental Tests*. Water, **12** (4): 1203.

Iverson R.M. (2015) - *Scaling and design of landslide and debris-flow experiments*. Geomorphology, **244**: 9-20.

Lienhart W. (2015) - *Case studies of high-sensitivity monitoring of natural and engineered slopes*. Journal of Rock Mechanics and Geotechnical Engineering, **7** (4): 379-384.

Martinelli M. & Ferrario M. (2013) - *Synoptic fiber optic sensor*. Patent W02013179118A1

Michlmayr G., Chalari A., Clarke A. & Or D. (2017) - *Fiber-optic high-resolution acoustic emission (AE) monitoring of slope failure*. Landslides, **14** (3): 1139-1146.

Papini M., Ivanov V.I., Brambilla D., Ferrario M., Brunero M., Cazzulani G. & Longoni L. (2020) - *First Steps for the Development of an Optical Fibre Strain Sensor for Shallow Landslide Stability Monitoring Through Laboratory Experiments*. In Applied Geology (197-208): Springer.

Picarelli L., Damiano E., Greco R., Minardo A., Olivares L. & Zeni L. (2015) - *Performance of slope behavior indicators in unsaturated pyroclastic soils*. Journal of mountain science, **12** (6): 1434-1447.

Prerau M.J., Brown R.E., Bianchi M.T., Ellenbogen J.M. & Purdon P.L. (2017) - *Sleep neurophysiological dynamics through the lens of multitaper spectral analysis*. Physiology, **32** (1): 60-92.

Rajan G., Jinachandran S., Xi J., Li H., Vinod J.S., Moses T. & Prusty B. G. (2016) - *Fibre optic acoustic emission measurement technique for crack activity monitoring in civil engineering applications*. Paper presented at the 2016 IEEE Sensors Applications Symposium (SAS).

Sbarufatti C., Beligni A., Gilioli A., Ferrario M., Mattarei M., Martinelli M. & Giglio M. (2017) - *Strain wave acquisition by a fiber optic coherent sensor for impact monitoring*. Materials, **10** (7): 794.

Scaioni M., Crippa J., Yordanov V., Longoni L., Ivanov V.I. & Papini M. (2018) - *Some tools to support teaching photogrammetry for slope stability assessment and monitoring. Int. Arch. Photogramm*. Remote Sens. Spatial Inf. Sci., XLII-3/W4: 453-460.

Schenato L. (2014) - *Fiber-optic sensors for geo-hydrological applications: Basic concepts and applications*. Rendiconti Online della Società Geologica Italiana, **30**: 51-54.

Schenato L. (2017) - *A review of distributed fibre optic sensors for geo-hydrological applications*. Applied Sciences, **7**: 896.

Smith A., Dixon N. & Fowmes G.J. (2017) - *Early detection of first-time slope failures using acoustic emission measurements: large-scale physical modelling*. Géotechnique, **67** (2): 138-152.

Smith A., Dixon N., Meldrum P., Haslam E. & Chambers J. (2014) - *Acoustic emission monitoring of a soil slope: Comparisons with continuous deformation measurements*. Géotechnique Letters, **4** (4): 255-261.

Thomson D.J. (1982) - *Spectrum estimation and harmonic analysis*. Proceedings of the IEEE, **70** (9): 1055-1096.

Received February 2021 - Accepted May 2021